NeuroImage: Clinical 35 (2022) 103051

Contents lists available at ScienceDirect

NeuroImage: Clinical

journal homepage: www.elsevier.com/locate/ynicl

Motor imagery in amyotrophic lateral Sclerosis: An fMRI study of postural control

Malek Abidi [a,b], Pierre-Francois Pradat [c,d,e], Nicolas Termoz [a,b], Annabelle Couillandre [a,f], Peter Bede [c,d,g], Giovanni de Marco [a,b,*]

[a] LINP2 Laboratory, UPL, Paris Nanterre University, France
[b] COMUE Paris Lumières University, France
[c] Department of Neurology, Pitié-Salpêtrière University Hospital, Paris, France
[d] Biomedical Imaging Laboratory, Sorbonne University, CNRS, INSERM, Paris, France
[e] Biomedical Sciences Research Institute, Northern Ireland Centre for Stratified Medicine, Ulster University, Londonderry, UK
[f] Université Paris-Saclay,CIAMS, Orsay, France
[g] Computational Neuroimaging Group, Trinity College Dublin, Ireland

ARTICLE INFO

Keywords:
ALS
Connectivity
Neuroimaging
Motor imagery
DCM
fMRI

ABSTRACT

Background: The functional reorganization of brain networks sustaining gait is poorly characterized in amyotrophic lateral sclerosis (ALS) despite ample evidence of progressive disconnection between brain regions. The main objective of this fMRI study is to assess gait imagery-specific networks in ALS patients using dynamic causal modeling (DCM) complemented by parametric empirical Bayes (PEB) framework.

Method: Seventeen lower motor neuron predominant (LMNp) ALS patients, fourteen upper motor neuron predominant (UMNp) ALS patients and fourteen healthy controls participated in this study. Each subject performed a dual motor imagery task: normal and precision gait. The Movement Imagery Questionnaire (MIQ-rs) and imagery time (IT) were used to evaluate gait imagery in each participant. In a neurobiological computational model, the circuits involved in imagined gait and postural control were investigated by modelling the relationship between normal/precision gait and connection strengths.

Results: Behavioral results showed significant increase in IT in UMNp patients compared to healthy controls ($P_{corrected} < 0.05$) and LMNp ($P_{corrected} < 0.05$). During precision gait, healthy controls activate the model's circuits involved in the imagined gait and postural control. In UMNp, decreased connectivity (inhibition) from basal ganglia (BG) to supplementary motor area (SMA) and from SMA to posterior parietal cortex (PPC) is observed. Contrary to healthy controls, DCM detects no cerebellar-PPC connectivity in neither UMNp nor LMNp ALS. During precision gait, bilateral connectivity (excitability) between SMA and BG is observed in the LMNp group contrary to UMNp and healthy controls.

Conclusions: Our findings demonstrate the utility of implementing both DCM and PEB to characterize connectivity patterns in specific patient phenotypes. Our approach enables the identification of specific circuits involved in postural deficits, and our findings suggest a putative excitatory–inhibitory imbalance. More broadly, our data demonstrate how clinical manifestations are underpinned by network-specific disconnection phenomena in ALS.

1. Introduction

Amyotrophic lateral sclerosis (ALS) is a progressive and fatal neuromuscular disease. The motor clinical picture of ALS is characterized by increasing spasticity, weakness, postural instability, backward falls, impaired postural reflexes, retropulsion, bradykinesia, and rigidity (Feron et al., 2018; Pradat et al., 2009). Numerous studies have investigated the neuronal substrate of motor and gait impairment in amyotrophic lateral sclerosis (ALS) and it is thought to be driven by multi-network degeneration affecting motor, extra-pyramidal and cerebellar circuits (Feron et al., 2018). Based on longitudinal functional studies, it had been postulated that despite relentless cerebral and spinal degenerative changes compensatory processes may occur during the course of ALS (Proudfoot et al., 2019). The study and characterization of

* Corresponding author at: 200 avenue de la République, 92000 Nanterre, France.
E-mail address: demarco.giovanni@gmail.com (G. de Marco).

https://doi.org/10.1016/j.nicl.2022.103051
Received 1 January 2022; Received in revised form 2 April 2022; Accepted 15 May 2022
Available online 17 May 2022
2213-1582/© 2022 The Author(s). Published by Elsevier Inc. This is an open access article under the CC BY-NC-ND license (http://creativecommons.org/licenses/by-nc-nd/4.0/).

adaptive functional processes may help to develop effective rehabilitation strategies and potentially slow functional decline. One of the key facets of clinical heterogeneity in ALS is the relative involvement of upper and lower motor neurons which defines the clinical phenotype, determines the disability profile of patients and ultimately their care needs.

The neuronal underpinnings of physiological gait and postural control have been successfully studied by functional magnetic resonance imaging (fMRI) and positron emission tomography (PET) using a motor imagery task (Jahn et al., 2008; la Fougère et al., 2010) which confirmed the pivotal role of the supraspinal locomotor network encompassing the supplementary motor area (SMA), the posterior parietal cortex (PPC), the basal ganglia (BG), and cerebellum. There is compelling evidence that imagined movements are largely analogous to executed movements with regard to intention, motor planning, and motor control (Marc Jeannerod, 2001) and both tasks result in similar activation patterns (M. Jeannerod, 1995). This analogy is crucial to study populations with considerable motor disability (Lulé et al., 2007).

The majority of motor imagery studies have focused on the extent of brain activation, and interaction within the motor system is poorly characterized. Several fMRI studies have used functional connectivity methods to investigate correlations between time series across the brain. They found functional alterations and large-scale brain networks disconnection. However, these correlational methods do not reveal the causal influence of one neural system on another (Friston, 2011). In order to overcome this methodological limitation, some authors have advocated for alternative approaches, such as the assessment of 'effective connectivity' which is defined as the directed (causal) influence of one (neuronal) system on another, which is inferred by modeling the neuronal interactions that generate BOLD time series (Friston et al., 1997). This generative approach, called dynamic causal modelling (DCM), is strongly hypothesis driven. Among all known effective connectivity methods such as structural equation modeling (SEM), multivariate autoregressive modeling (MAR) and Granger causality (GC), DCM is a well-established determinist method permitting the modeling of causal influences among different brain regions (Friston et al., 2003). By modeling time-varying hidden parameters that affect the transformation of neuronal activity into a hemodynamic response, DCM estimates the temporal precedence of one neuronal system over another and assesses how changes in one system linearly and nonlinearly influence another, how changes in multiple systems influence each other across time and how those neural interactions are influenced by external perturbations.

In this fMRI study, we aimed to investigate neural interactions in the motor system during imagery to characterize hemodynamic responses in a cohort of clinically stratified ALS patients. We hypothesized that implementing state-of-the-art models such as DCM, we will succeed in describing effective connectivity patterns within a large-scale brain network, including the gait circuits. This is in sharp contrast with the method of the psychophysiological interactions (PPI), which operates at the level of the measured BOLD signal and focuses on a single source region. The evaluation of a single seed region limits the extent to which one can infer causal relationships in the brain, making the interpretation of the interactions ambiguous. Furthermore, the absence of a forward model linking neuronal activity to the measured haemodynamic BOLD signals makes analyses of inter-regional connectivity by PPI problematic.

The advantage of DCM is that the coupling between models of neural dynamics and biophysical forward models is a mandatory component (Friston et al., 2011). Moreover, this causal method offers new insights into the pathophysiology of neurological disease and potentially into pharmacodynamics (Rowe et al., 2010). Accordingly, our objective is to investigate the effective connectivity with DCM, among four key motor regions: the supplementary motor area, the posterior parietal cortex, the cerebellum and the basal ganglia, which are known to closely interact during motor-imagery of gait (Abidi et al., 2021; Bakker et al., 2008; la Fougère et al., 2010). Using a plausible neurobiological model of imagined gait, our study aims to capture phenotype-specific connectivity patterns within the gait control and postural control circuits in ALS. Our overarching objective is the demonstration of differential network degeneration in clinical phenotypes and showcase the utility of imagery based paradigms in studying patient cohorts with significant motor disability.

2. Materials and methods

2.1. Subjects

This study was approved by the institutional research board of the CPP Ile-de-France Paris VI. Thirty-one patients with ALS and 14 age- and gender-matched healthy controls gave informed consent to participate in this study. Based on standardized clinical evaluation (Simon et al., 2015), ALS patients were divided into two subgroups: a UMNp cohort (n = 14) and an LMNp group (n = 17) (Table 1). Clinically, UMNp patients exhibited frank UMN predominance based on established UMN signs, such as marked spasticity, Hoffmann sign, Babinski sign, clonus etc. UMN burden was estimated based on the revalidated Penn UMN score (Quinn et al., 2020). LMNp patients showed obvious clinical signs of LMN pathology predominance such as decreased tone, muscle atrophy, fasciculations etc. Inclusion criteria included 'definite' or 'probable' ALS according to the revised El Escorial criteria (Brooks et al., 2000), age between 18 and 70 years, right-handedness. Exclusion criteria included frank frontotemporal dementia based on the Rascovsky criteria, comorbid musculoskeletal conditions that would have interfered with functional evaluation, and contraindications to MRI.

All participants underwent a standardized clinical examination on the day of imaging. Functional impairment was evaluated by the revised ALS Functional Rating Scale (ALSFRS-r). Disease progression rate was calculated as ((48-ALSFRS-r)/disease duration in months). All participants also underwent a comprehensive neuropsychological evaluation including tests for memory, executive, language and visio-spatial domains (Table 1).

2.2. Motor imagery paradigm

The paradigm consisted of two tasks: a motor imagery (MI) task and a visual imagery (VI) task. Both tasks were tested with normal locomotion (broad path) and with complex locomotion (narrow path). A total of four photographs were used for the experimental procedure (i.e., two start pads × two path widths). Subjects were asked to observe the photograph for 3 s and then they were asked to imagine performing the task while keeping their eyes closed.

Participants were given written instructions before the training sessions and the fMRI experiment. On the day of the scan, the instructions were explained again, and a practice session was organized outside the scanner to simulate the procedure before data acquisition commenced inside the scanner.

During the MI task, subjects were asked to imagine walking along the path in an egocentric perspective called "first person." However, during the VI task participants had to imagine observing a black disc moving along the trajectory. The VI was used as a control condition (Fig. 1).

2.3. Motor imagery scores: The visual and kinesthetic scales

Computation of mean scores (average, standard deviation [SD]) was carried out for each scale VI and KI in each group. The resultant values may vary from 1 to 7, with a score of 7 constituting maximal motor imagery ability. The 2 × 3 repeated-measures ANOVA compared VI and KI scores between groups and were carried out using Statistica 13.0 software. $P < 0.05$ was considered significant.

Table 1
The demographic and clinical profile of study participants.

	Healthy controls (n = 14)	UMN predominant ALS patients (n = 14)	LMN predominant ALS patients (n = 17)	*p* value
Age (years)	63.0 (57.0–66.0)	59.0 (20.0–71.0)	62.0 (31.0–74.0)	0.39
Sex (female/ male)	5/9	3/10	6/11	0.29
Height (cm)	170 (168–175)	171 (157–187)	176 (154–186)	0.34
Weight (kg)	74.5 (66.0–83.7)	67.2 (53.0–90.0)	66.0 (54.0–86)	0.45
Disease Onset				
Upper limb	NA	3	3	0.37
Lower limb		7	10	0.58
Bulbar		4	4	0.81
ALSFRS-r (max. 48)	NA	37.5(35.2–41.0)	40.0 (33.0–46.0)	0.07
Disease duration (months)	NA	23.5(14.7–37.2)	15.0 (07.0–80.0)	0.73
Disease progression rate	NA	0.58(0.12–1.1)	0.46 (0.09–1.0)	0.13
Cognitive assessment				
California verbal learning test II CVLT II				
Immediate recall	NA	07.0 (04.0–13.0)	06.0 (04.0–10.0)	0.16
total trial recall (1–5)		57.0 (35.0–68.0)	52.0 (38.0–69.0)	0.32
Short delay free recall		12.0 (09.0–16.0)	12.0 (07.0–16.0)	0.21
Short delay cued recall		01.0 (0–13.0)	02.0(0–16.0)	0.48
Long delay free recall		14.0 (11.0–16.0)	14.0 (09.0–16.0)	0.41
Long delay cued recall		01.0 (0–13.0)	01.0 (0–16.0)	0.25
Total recognition discrimination		16.0 (13.0–16.0)	16.0 (0–16.0)	0.27
Stroop test				
Reading	NA	99.5 (46.0–117)	92.0 (41.0–123.0)	0.23
Naming		73.5 (34.0–84.0)	64.0 (40.0–80.0)	0.13
Double task		38.5 (24.0–53.0)	37.0 (17.0–50.0)	0.33
Verbal fluency test				
Phonemic	NA	25.0 (03.0–40.0)	18.0 (09.0–38.0)	0.46
Semantic		31.0 (16.0–51.0)	32.0 (10.0–45.0)	0.44
Wisconsin card sorting test				
Categories achieved	NA	06.0 (01.0–06.0)	06.0 (03.0–06.0)	0.36
Perseverative errors		07.0 (0–31.0)	09.5 (05.0–17.0)	0.22
		03.0 (0–11.0)	04.0 (01.0–09.0)	0.38
Digit span				
Forward	NA	08.0 (04.0–11.0)	07.0 (04.0–13.0)	0.49
Backwards		05.0(04.0–08.0)	04.0 (02.0–10.0)	0.34

2.4. Acquisition of behavioral data

For each trial, the time between the two button presses that marked the start and the end of the imagined visual or motor conditions (imagery time [IT]) was recorded. Furthermore, the effects of task (motor imagery [MI], visual imagery [VI]) and path width (narrow, wide) on the response time in each group were also assessed.

2.5. MRI data acquisition

MRI data were acquired with a 3 T Siemens (Erlangen, Germany) Prisma platform using a 32-channel head coil. T1-weighted structural images were acquired with a magnetization-prepared rapid acquisition-gradient echo (MP-RAGE) sequence with a repetition time (TR) / echo time (TE) = 2300/4.2 ms, inversion time (TI) = 900 ms, and isotropic 1 × 1 × 1 mm voxel size. Functional images were obtained using a single-shot gradient echo (GE-EPI) sequence. A total of 700 EPI volumes were acquired with TR/TE = 2020/27 ms; flip angle = 78; field of view (FOV) = 198 × 198 mm2 for the motor paradigm using 3 mm slice thickness.

2.6. fMRI data preprocessing and experimental conditions

Functional MRI analyses were performed using the Statistical Parametric Mapping SPM12 (https://www.fil.ion.ucl.ac.uk/spm/). In each dataset, for T1 equilibrium, the first four volumes were discarded. All EPI volumes were corrected to adjust for within-volume time differences and then realigned with the last volume to correct for head movements. The fMRI data were coregistered with the T1 anatomical images of the same subject and then spatially normalized into the MNI space. Spatial smoothing was performed with an 8-mm full width half-maximum Gaussian kernel. A whole-brain analysis was performed using the motor imagery broad (MI-Broad) condition to identify the brain regions involved in imagined locomotion of normal gait. A complementary analysis measuring the specific effects of the trajectory constraints was also carried out using the motor imagery-narrow (MI-Narrow) condition. This condition aimed to identify brain areas more specifically involved in postural control and balance during complex imagined locomotion.

2.7. Region of interest selection for DCM

Four regions of interest (supplementary motor area, cerebellum, basal ganglia and posterior parietal cortex) were defined on the basis of prior knowledge of their functional interaction in motor imagery and on the basis of their activation in the second-level random-effect SPM analysis. Anatomical masks of the SMA, cerebellum, basal ganglia and PPC were created using the Automated Anatomical Labeling (AAL) atlas of the SPM Wake Forest University (WFU) PickAtlas toolbox and placed in each subject. The cerebellar mask included lobule VI and crus I/II of the cerebellum, and the basal ganglia mask included putamen and caudate. Time series were extracted, pre-processed and summarized within each ROI by their first principal component.

2.8. DCM approach

Effective connectivity analysis was performed using dynamic causal modelling (Friston et al., 2003), as implemented in SPM12, to link all these regions in the same model by considering different commonalities of connectivity. The underlying principle behind DCM is that it considers the brain as a non-linear dynamical system where inputs are known along with experimental perturbations (Friston et al., 2003). DCM is a framework for specifying, estimating and comparing generative models of time series. It incorporates known effects of interest and assesses task-dependent modulations among a group of interconnected regions through a set of matrices, known as: (a) task independent endogenous connectivity (matrix A) among the regions representing influence without any external perturbation, (b) task dependent modulation effects (matrix B) representing changes in endogenous connection strength due to external perturbations and (c) direct influence of an external input (driving input) to a region (matrix C) (Friston et al., 2003; Pool et al., 2013). In addition to interactions between regions, DCM allows for external stimuli to influence regions, either directly or by modifying the connections between regions.

We hypothesized that the average strengths of endogenous and

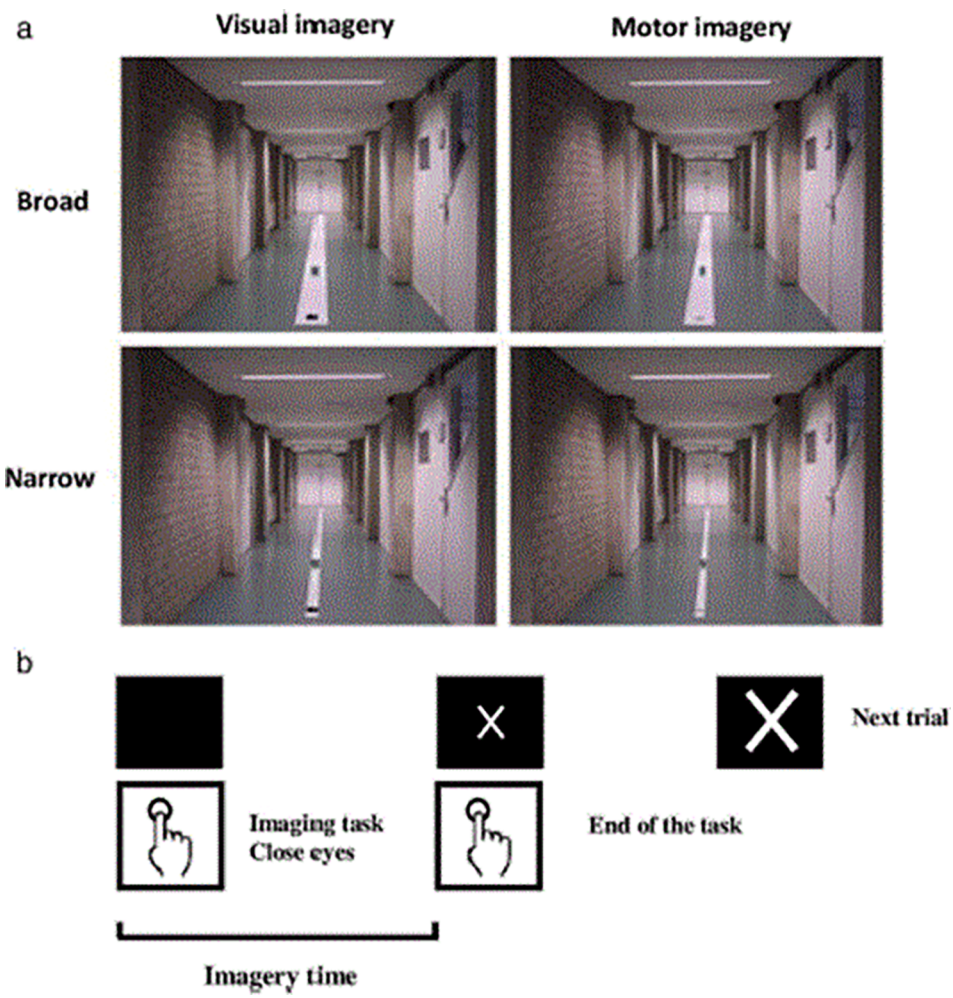


Fig. 1. The experimental protocol based on the Bakker study (Bakker et al., 2008) Subjects were asked to perform a mental imagery task in either motor (MI) or visual (VI) mode depending on presented visual stimulus (photos). During MI trials, a green square is present at the beginning of the path. During VI trials, a black disc is shown at the beginning of the path. The end of the path was identical irrespective of the imaging task (visual and motor), and was represented by a green pad displayed at a fixed distance of 6 m. (a) The photos show a corridor with a white path in the middle and a green sign positioned on the path. (b) Time-course of the experiment, participants were asked to close their eyes while imagining themselves standing, and to press the button when they started imagining walking on the path and to press the button again at the end of the task. The inter-trial interval was random (4 to 12 sec). The transition to the next test was signaled by the appearance of a large "X" sign in the center of the screen.

modulatory connectivity would be unique to the study-groups and change according to width path conditions. Our neural model was specified with bidirectional connections between all regions (SMA, basal ganglia, PPC and cerebellum, except the PPC-basal ganglia circuit as this connection doesn't play a crucial role in imagined gait. This base model was then modified systematically to produce ten plausible alternative models' variants determined after Bayesian Model reduction described below.

2.9. Parametric empirical Bayes (PEB) analysis

To enable the quantification of commonalities and differences across subjects (inter-subject variability) in neural circuitry, DCM is supplemented with a hierarchical model over parameters, called the Parametric Empirical Bayes (PEB) framework (Friston et al., 2016). The PEB approach estimates the effect of each covariate on each connection (both the group mean and any group differences), as well as determining between-subject variability. The parameters of the PEB model were computed using a standard variational Laplace procedure. After having fitted each subject's DCM to their data, we subsequently performed PEB analysis to estimate the group mean and the effect of path width (broad versus narrow) on each connection within each group.

2.10. Bayesian model comparison (BMC)

To evaluate how the connectivity in broad band condition differs from that in narrow band condition, we used Bayesian model comparison to explore the space of possible models, where each model assumes that a different combination of the connections could exist across participants. It refers to the process of comparing the evidence of the full GLM model with multiple reduced GLM models that have certain combinations of connectivity parameters switched off, by fixing the prior expectation at zero (Zeidman et al., 2019). Such comparisons are very efficient since the evidence and parameters of reduced PEB models can be derived analytically from the full model using Bayesian Model Reduction (Friston et al., 2016). Lastly, to confirm the Bayesian Model Comparison results, we applied Bayesian Model Reduction to automatically remove redundant effective connectivity links from the full PEB model that did not contribute to the model evidence. Specifically, the algorithm implemented a greedy searching over all the permutations of a small set of parameters (i.e., twenty four parameters in our case) whose removal produces the smallest reduction (i.e., greatest increase) in model fitting (Friston et al., 2003). The procedure was repeated until discarding any parameter starts to decrease model evidence or there were no more new parameters to add. After Bayesian Model Reduction, the best ten reduced models were combined by using Bayesian Model Averaging to account for uncertainty about the underlying model.

In summary the main steps of PEB analysis include 1) specifying a DCM for each subject 2) fitting it to their data, providing estimates of the connectivity parameters (expected values and covariance) 3) subject-specific estimates are taken to group-level and modeled using a Bayesian approach of the GLM (PEB model) 4) the parameters of the GLM represent the group average of each connectivity parameter and group differences 5) using a Bayesian model reduction to search over the reduced PEB models with different combinations of connections 6) the best models from this search were combined using Bayesian model

averaging whose results are reported below.

3. Results

3.1. Behavioral results

The UMNp and LMNp groups were matched in age, ALSFRS-r subscores, disease duration, progression rates, and cognitive performance. No significant inter-group difference were detected in the MIQ-RS F(2, 42) = 1.13, P = 0.33. Visual and kinesthetic scores were high (KI: mean = 5.04, SD = 1.23; VI: mean = 5.71, SD = 0.96) indicating a good imagery ability in each group.

A significant main effect of path width on imagery time (IT) was observed in the MI task (F(1, 42) = 67.76, P < 0.05; effect size: partial η2 = 0.61). The IT systematically increased with decreasing path width. On the other hand, path width had no significant effect on the IT of visual imagery F(1, 42) = 0.13, P = 0.71). A Group–Band interaction was also observed (F(2, 42) = 13.50, P = <0.05; effect size: partial η2 = 0.38). After Bonferroni correction (tests post-hoc), UMNp patients had longer IT on the narrow path compared to control subjects (P < 0.05) and LMNp patients (P < 0.05). No significant difference was observed between the control subjects and LMNp patients on the narrow path.

3.2. Effective connectivity results

3.2.1. Healthy control group

Endogenous connection strengths in controls revealed significant connectivity between all the model nodes (Fig. 2) with bilateral connections which demonstrates the neurobiological plausibility of the model. In contrast, for the broad path condition, BG → SMA effective connectivity was positively modulated. A negative bilateral connectivity between BG → Cerebellum (−0.040) and Cerebellum → BG (−0.037) was observed, suggesting a decrease or suppression of these connections during broad path condition in control group (Table 2, Fig. 3).

During Narrow path condition, we observe in controls significant connectivities within SMA → PPC and Cerebellum → PPC. A similar positive bilateral connectivity between BG → Cerebellum and Cerebellum → BG was also recorded suggesting activation (excitation) of these connections with increased postural control processing (Table 2, Fig. 4).

3.2.2. LMN group

Endogenous connection strengths in LMN patients revealed significant connectivities between all the nodes of the model (Fig. 2). As controls, for the broad path condition, LMN patients present significant positive connectivity between BG → SMA and similar negative bilateral effective connectivity between BG and cerebellum. The bilateral inhibition of BG and cerebellum connectivity suggests a lesser involvement of this circuitry in broad path condition (Table 2, Fig. 3). During narrow path condition, LMN patients present different pattern of connectivity as healthy controls. Significant effective connectivity between SMA → PPC and positive bilateral connectivity between BG and Cerebellum was recorded. However, significant bilateral SMA-basal ganglia interaction and suppression of cerebellum –>PPC connectivity was observed (table2; Fig. 4).

3.2.3. UMN group

Endogenous connection strengths in UMN patients revealed significant connectivity in all the model nodes (Fig. 2). In contrast, for the broad path condition, BG → SMA and SMA → PPC effective connectivity were negatively modulated by broad path condition. Negative effective connectivity between these regions was detected suggesting an inhibition of these connections during broad path condition (table 2, Fig. 3). Different pattern of activations/connections were demonstrated in UMN patients during narrow path condition. Only a positive bilateral effective connectivity between BG and Cerebellum was recorded (table2, Fig. 4).

4. Discussion

This study investigated the effective integrity of the motor network during motor imagery of locomotion in ALS. We have successfully applied DCM to fMRI data on imagined gait and were able to

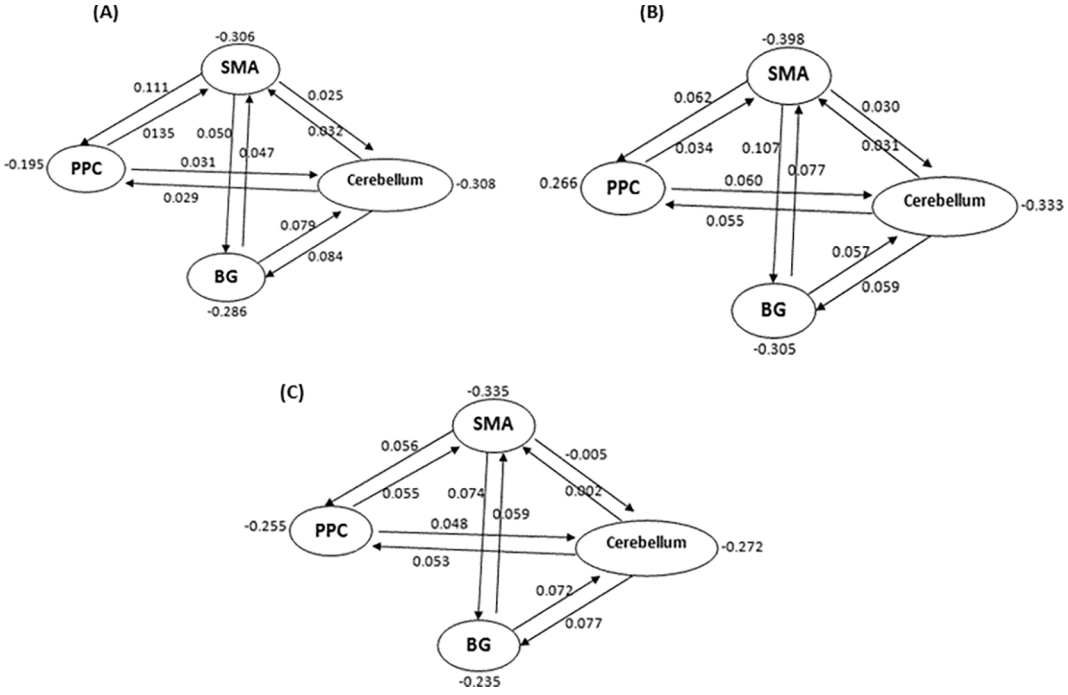


Fig. 2. The average strength of endogenous connectivity parameters for Controls (A), LMN (B) and UMN (C). The values (coupling parameters) reflect a rate constant (Hz) at which activity is propagated from one region to another. Values are significant at a posterior probability >95%. SMA = Supplementary motor area; PPC = Posterior parietal cortex; BG = Basal Ganglia.

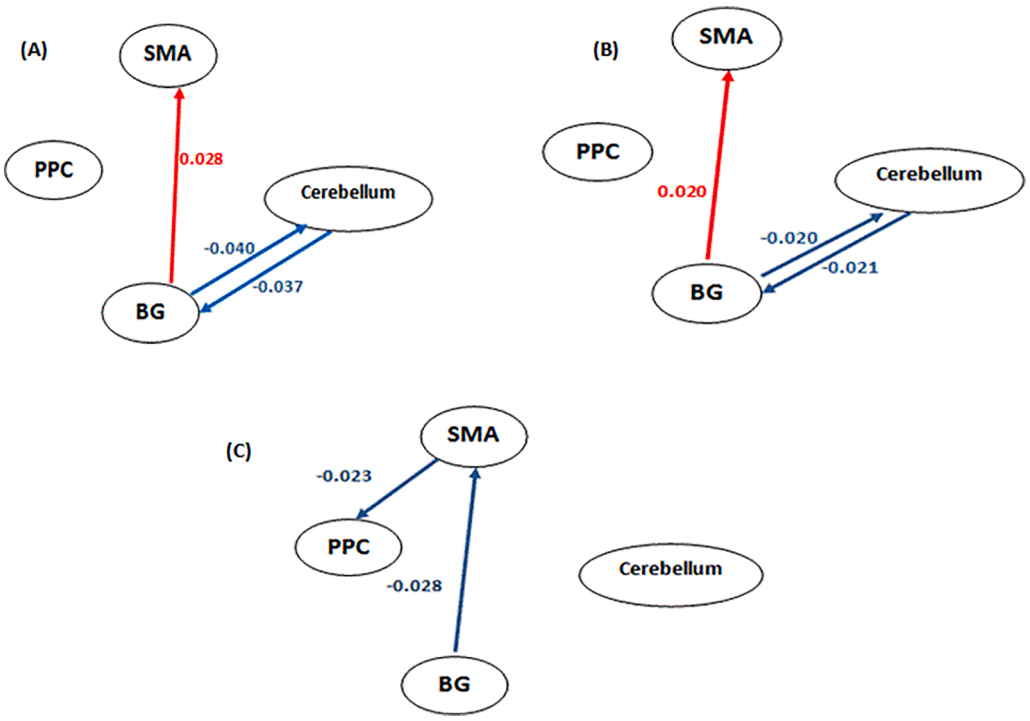


Fig. 3. Effective connectivity during broad path condition within control (A), LMN (B) and UMN (C). The red line represents increased connectivity and the blue lines represent decreased connectivity.

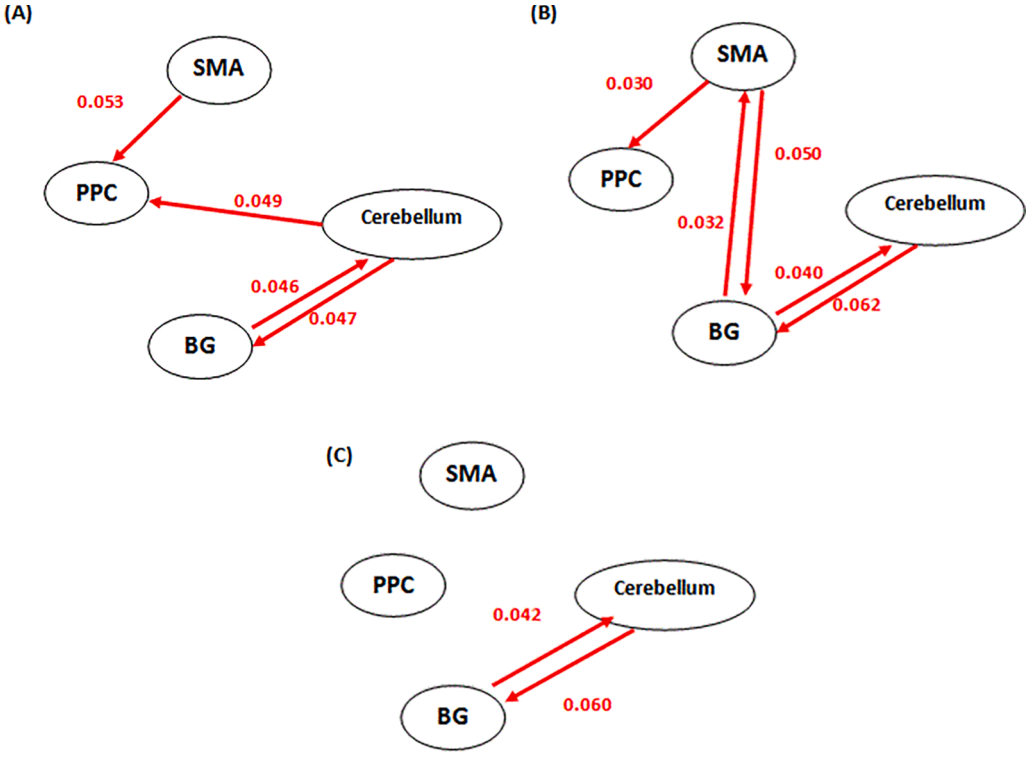


Fig. 4. Effective connectivity during narrow path condition within control (A), LMN (B) and UMN (C). The red lines represent increased connectivity.

characterize distinct patterns of effective connectivity during normal and precision gait tasks in both UMNp and LMNp ALS patients.

There is ample imaging evidence of structural disconnection between cortical and sub-cortical regions in ALS (Bede et al., 2018, 2021; Meier et al., 2020; Tu et al., 2018), but the functional interplay between these structures has not been characterized in sufficient detail. Our results revealed increased effective connectivity between basal ganglia and cerebellum and decreased connectivity between basal ganglia- SMA and SMA-PPC in UMNp patients during imagined gait. This reported increase between basal ganglia and cerebellum may be driven by the increased inhibitory influences from SMA to PPC and basal ganglia to SMA. This finding provides a possible novel explanation for the

Table 2
The average strength of modulatory connectivity parameters in Healthy controls, LMN,UMN in broad and narrow path condition. Values in bold are significant at a posterior probability >75%.

		Broad path condition				Narrow path condition			
		SMA	PPC	BG	Cerebellum	SMA	PPC	BG	Cerebellum
Healthy controls	SMA		−0.007	**0.028**	0.010		0.027	0.014	−0.030
	PPC	0.008			−0.015	**0.053**			**0.049**
	BG	−0.004			**−0.037**	0.014			**0.047**
	Cerebellum	0.012	−0.008	**−0.040**		−0.016	−0.004	**0.046**	
LMN	SMA		−0.0007	**0.020**	0.007		0.017	**0.032**	0.0009
	PPC	0.006			0.008	**0.030**			0.007
	BG	0.003			**−0.020**	**0.050**			**0.062**
	Cerebellum	0.001	−0.002	**−0.021**		−0.008	0.008	**0.040**	
UMN	SMA		−0.0069	**−0.028**	−0.0092		0.0149	0.0092	0.0001
	PPC	**−0.0237**			0.0091	0.0024			0.0178
	BG	−0.0065			−0.0067	0.0160			**0.0607**
	Cerebellum	0.0073	−0.0015	−0.015		−0.0079	0.0099	**0.0425**	

SMA; Supplementary Motor Area, PPC; Posterior Parietal Cortex, BG; Basal Ganglia.

commonly observed increased connectivity in sub-cortical areas in ALS patients (Abidi et al., 2020; Abidi et al., 2021; Tessitore et al., 2006). PPC is known to store representations of movement and predict conscious motor intentions (Assal et al., 2007), whereas SMA will reflect the imminence of a motor response (Desmurget et al., 2009). The integrity of premotor-parietal and subcortical-SMA connectivity is essential to process visuospatial stimulus without the execution of motor motion (Cavanna & Trimble, 2006) and is crucial in locomotion, balance adjustments, and maintaining posture (Bakker et al., 2008; Jahn et al., 2008). The PPC was specifically implicated in gait studies due to its connectivity with motor and premotor cortices (Niedermeyer et al., 2004), and other studies have also suggested its role in complex sensorimotor processing (Tjernström et al., 2010). The PPC has been proposed to generate a body schema that would be responsible for integrating limb movement, and their movements relative to the body, integrating information about the surrounding environment (Takakusaki et al., 2008). The activation of the PPC for sensory integration, body schema, error monitoring and adjusting movement to environmental constraints would allow the PPC to assist the SMA in selecting subsequent locomotor plan updates Hinton et al., 2019). The negative association (inhibition) between premotor and posterior parietal areas indicates that UMNp ALS patients are unable to bring these brain regions online, leading to increasing gait imagining time and altering movement. These results are in accordance with previous findings within traumatic brain injury patients, in which authors demonstrated decreased premotor-parietal connectivity during postural control task and this decrease in connectivity degree was significantly associated with poorer balance performance (Caeyenberghs et al., 2012).

A multitude of studies have demonstrated how pontine and mesencephalic locomotor regions control postural muscle tone and coordinate stepping movements (Musienko et al., 2012). These regions are known to the affected in ALS (Bede et al., 2019). They receive projections from the SMA (Matsumura et al., 2000), and inhibition of the SMA disturbs locomotor regions functions and alters postural control (Mori & Nakajima, 2010). Accordingly, it seems that the inhibitory influence of the basal ganglia to SMA in UMNp patients leads to altered connections between SMA and brainstem, the pons, and the mesencephalic locomotor region which affect postural control, balance and gait.

Consequently, impaired SMA-PPC and BG-SMA connectivity was associated with increased BG-cerebellar interaction within UMNp patients. The massive recruitment of this subcortical circuitry may represent a compensatory mechanism activated due to limited resources of premotor cortex. The basal ganglia and cerebellum are two groups of subcortical nuclei that are highly implicated in motor control as well as in cognitive functions processing (Belkhiria et al., 2017). Damage to these brain regions produces well-described alterations in motor and cognitive functions (Middleton & Strick, 2000). A multitude of studies have provided evidence that the basal ganglia and the cerebellum are not independent systems but, form a closely interconnected network (Bostan et al., 2010). Thus, changes at one node can percolate throughout the entire network to influence operations at other nodes (Bostan et al., 2010). The cerebellum contains neural representations reproducing the dynamic properties of the body and to exploit them to create sensorimotor predictions; this allows performing accurate motor forecasts linked to environmental stimuli/constraints and to body kinematics (Manto & Huisman, 2018). The wide neural network in which the cerebellum communicates with the basal ganglia allows not only movement prediction, coordination and timing but also the definition of spatiotemporal and visuospatial sequences of body segment movements and the generation of appropriate patterns of limb movements and in modulating their activation duration during locomotion (Martino et al., 2014).

Our study managed also to show an absence of cerebellum-PPC connection in UMNp patients during narrow path condition compared to controls. Both regions are thought to be critically involved in postural adjustments, balance control, and motor coordination (Goel et al., 2019), as well as the prediction of sensory consequences of action (Blakemore et al., 2003). These predictions contribute to limb positioning and negotiating environmental constraints (Bakker et al., 2008). During locomotion, cerebellar climbing fibers increase their activity, coding for predicted error severity during the stance portion of the perturbed leg and the swing phase of the next step and allowing for planning of the next foot placement (Yanagihara & Udo, 1994). The activation of PPC would then complement feedback from cerebellum to inform updates to the locomotor plan and allow an associative workload needed to integrate visual and proprioceptive stimuli (Hinton et al., 2019). Reciprocal connection between cerebellum and PPC is then critically involved in encoding internal postural model in space and self-motion (Shaikh et al., 2004). Such a bodily information can be utilized to maintain upright posture during standing and to achieve anticipatory postural adjustment (Takakusaki, 2017). Therefore, damage observed in UMNp within the cerebellar—PPC connection makes gait adaptation to environment constraints impossible.

More interestingly, this damage was also recorded in LMNp patients, however, these latter, compared to healthy controls and UMNp patients, present additional connectivity between SMA and basal ganglia to probably compensate the suppression of cerebellum-PPC connection. Previous researches highlight the crucial role of the SMA-basal ganglia connection in locomotion especially in motor imagery task. Cortical commands for locomotion originate in the supplementary motor cortices and are conveyed by the basal ganglia to brainstem locomotor centers (Bakker et al., 2008; Jahn et al., 2008; la Fougère et al., 2010). In addition, it has been shown that the SMA was highly activated when the task involved walking over obstacles rather than walking normally

(Malouin et al., 2003). This implies that this premotor region plays an important role in demanding balance tasks. Similarly, the basal ganglia are known to play an important role in balance and postural control for instance, they enable postural flexibility and sensorimotor integration (Visser & Bloem, 2005), in particular during complex gait task. These data highlight the role of the basal ganglia-SMA circuit in adapting the locomotor pattern in complex gait situations, and their probable dysfunction in pathological conditions could affect the ability to freely walk in complex environments (Maidan et al., 2016). Since previous research usually didn't capture any differences between LMNp patients and healthy controls (Abidi et al., 2020; Abidi et al., 2021; Tessitore et al., 2006), further researches are needed.

The nuanced characterization of the functional interplay between the cortex, basal ganglia and cerebellum has practical relevance to our understanding of gait impairment, fall risk and extrapyramidal features in ALS. While ALS is primarily associated with UMN and LMN degeneration, extrapyramidal involvement is a likely contributor to the heterogeneity of motor manifestations observed clinically. Beyond their contribution to motor disability, functional alterations between subcortical structures, the cerebellum and cortex are likely to drive ALS-associated cognitive and behavioral symptoms (Burke et al., 2016; Christidi et al., 2019).

This study is not without limitations. Although differences were detected in the locomotion network in ALS patients, future studies need to replicate and validate these findings in a larger sample of patients. Moreover, additional structural connectivity analyses would have complemented our functional connectivity findings to provide a more comprehensive and multifaceted characterization of network disintegration in ALS.

5. Conclusions

Our data provide evidence of functional reorganization and neural circuitry disconnection in UMN-predominant ALS patients and indicate that loss of network integrity is a key determinant of clinical manifestations. UMN-predominant ALS patients exhibit increased effective connectivity between cerebellum and basal ganglia and diminished BG-SMA and SMA-PPC connectivity during motor imagery of gait; which impacts on locomotor, balance and postural control processing. Enhanced basal ganglia-cerebellar connectivity may represent functional adaptation. We have identified a unique connectivity pattern in LMNp patients with enhanced SMA-BG connectivity which may counterbalance the lack of cerebellum-PPC connectivity during precision gait paradigms.

CRediT authorship contribution statement

Malek Abidi: Conceptualization, Methodology, Software, Data curation, Writing – original draft, Investigation, Formal analysis, Writing – review & editing. **Pierre-Francois Pradat:** Writing – review & editing. **Nicolas Termoz:** Writing – review & editing. **Annabelle Couillandre:** Writing – review & editing. **Peter Bede:** Writing – review & editing. **Giovanni de Marco:** Conceptualization, Methodology, Software, Data curation, Writing – original draft, Supervision, Validation, Writing – review & editing.

Declaration of Competing Interest

The authors declare that they have no known competing financial interests or personal relationships that could have appeared to influence the work reported in this paper.

Acknowledgments

We express our gratitude to all participating patients and each healthy control for supporting this research study. Without their contribution this study would not have been possible.

Funding

This study was funded by a grant from the Association for Research on ALS (ARSLA) and the Institut National pour la Santé et la Recherche Médicale (INSERM). The research leading to these results has also received support from the programme "Investissements d'avenir" (ANR-10-IAIHU-06). Professor Bede is supported by the Health Research Board, Ireland (HRB EIA-2017-019 and HRB JPND-Cofund2-2019-1), the Spastic Paraplegia Foundation, Inc. (SPF), the EU Joint Programme – Neurodegenerative Disease Research (JPND), and the Iris O'Brien Foundation.

References

Abidi, M., Marco, G., Couillandre, A., Feron, M., Mseddi, E., Termoz, N., Querin, G., Pradat, P.-F., Bede, P., 2020. Adaptive functional reorganization in amyotrophic lateral sclerosis: coexisting degenerative and compensatory changes. Eur. J. Neurol. 27 (1), 121–128.

Abidi, M., Marco, G., Grami, F., Termoz, N., Couillandre, A., Querin, G., Bede, P., Pradat, P.-F., 2021. Neural correlates of motor imagery of gait in amyotrophic lateral sclerosis. J. Magn. Resonance Imaging 53 (1), 223–233.

Assal, F., Schwartz, S., Vuilleumier, P., 2007. Moving with or without will: functional neural correlates of alien hand syndrome. Ann. Neurol. 62 (3), 301–306.

Bakker, M., De Lange, F.P., Helmich, R.C., Scheeringa, R., Bloem, B.R., Toni, I., 2008. Cerebral correlates of motor imagery of normal and precision gait. NeuroImage 41 (3), 998–1010.

Bede, P., Chipika, R.H., Christidi, F., Hengeveld, J.C., Karavasilis, E., Argyropoulos, G.D., Lope, J., Li Hi Shing, S., Velonakis, G., Dupuis, L., Doherty, M.A., Vajda, A., McLaughlin, R.L., Hardiman, O., 2021. Genotype-associated cerebellar profiles in ALS: focal cerebellar pathology and cerebro-cerebellar connectivity alterations. J. Neurol. Neurosurg. Psychiatry 92 (11), 1197–1205.

Bede, P., Chipika, R.H., Finegan, E., Li Hi Shing, S., Doherty, M.A., Hengeveld, J.C., Vajda, A., Hutchinson, S., Donaghy, C., McLaughlin, R.L., Hardiman, O., 2019. Brainstem pathology in amyotrophic lateral sclerosis and primary lateral sclerosis: a longitudinal neuroimaging study. NeuroImage: Clinical 24, 102054.

Bede, P., Omer, T., Finegan, E., Chipika, R.H., Iyer, P.M., Doherty, M.A., Vajda, A., Pender, N., McLaughlin, R.L., Hutchinson, S., Hardiman, O., 2018. Connectivity-based characterisation of subcortical grey matter pathology in frontotemporal dementia and ALS: a multimodal neuroimaging study. Brain Imaging Behav. 12 (6), 1696–1707.

Belkhiria, C., Driss, T., Habas, C., Jaafar, H., Guillevin, R., de Marco, G., 2017. Exploration and identification of cortico-cerebellar-brainstem closed loop during a motivational-motor task: an fMRI study. Cerebellum 16 (2), 326–339.

Blakemore, S.-J., Oakley, D.A., Frith, C.D., 2003. Delusions of alien control in the normal brain. Neuropsychologia 41 (8), 1058–1067.

Bostan, A.C., Dum, R.P., Strick, P.L., 2010. The basal ganglia communicate with the cerebellum. Proc. Natl. Acad. Sci. USA 107 (18), 8452–8456.

Brooks, B.R., Miller, R.G., Swash, M., Munsat, T.L., 2000. El Escorial revisited: revised criteria for the diagnosis of amyotrophic lateral sclerosis. Amyotrophic Lateral Sclerosis 1 (5), 293–299.

Burke, T., Pinto-Grau, M., Lonergan, K., Elamin, M., Bede, P., Costello, E., Hardiman, O., Pender, N., Cereda, C., 2016. Measurement of social cognition in amyotrophic lateral sclerosis: a population based study. PLoS One 11 (8), e0160850.

Caeyenberghs, K., Leemans, A., De Decker, C., Heitger, M., Drijkoningen, D., Linden, C. V., Sunaert, S., Swinnen, S.P., 2012. Brain connectivity and postural control in young traumatic brain injury patients: a diffusion MRI based network analysis. NeuroImage: Clinical. 1 (1), 106–115.

Cavanna, A.E., Trimble, M.R. (2006). The precuneus: a review of its functional anatomy and behavioural correlates. *Brain* https://doi.org/10.1093/brain/awl004.

Christidi, F., Karavasilis, E., Rentzos, M., Velonakis, G., Zouvelou, V., Xirou, S., Argyropoulos, G., Papatriantafyllou, I., Pantolewn, V., Ferentinos, P., Kelekis, N., Seimenis, I., Evdokimidis, I., Bede, P., 2019. Hippocampal pathology in amyotrophic lateral sclerosis: selective vulnerability of subfields and their associated projections. Neurobiol. Aging 84, 178–188.

Desmurget, M., Reilly, K.T., Richard, N., Szathmari, A., Mottolese, C., Sirigu, A., 2009. Movement intention after parietal cortex stimulation in humans. Science 324 (5928), 811–813.

Feron, M., Couillandre, A., Mseddi, E., Termoz, N., Abidi, M., Bardinet, E., Delgadillo, D., Lenglet, T., Querin, G., Welter, M.-L., Le Forestier, N., Salachas, F., Bruneteau, G., del Mar Amador, M., Debs, R., Lacomblez, L., Meininger, V., Pélégrini-Issac, M., Bede, P., Pradat, P.-F., de Marco, G., 2018. Extrapyramidal deficits in ALS: a combined biomechanical and neuroimaging study. J. Neurol. 265 (9), 2125–2136.

Friston, K.J., Buechel, C., Fink, G.R., Morris, J., Rolls, E., Dolan, R.J., 1997. Psychophysiological and modulatory interactions in neuroimaging. NeuroImage 6 (3), 218–229.

Friston, K.J., Harrison, L., Penny, W., 2003. Dynamic causal modelling. NeuroImage 19 (4), 1273–1302.

Friston, K.J., Li, B., Daunizeau, J., Stephan, K.E., 2011. Network discovery with DCM. NeuroImage 56 (3), 1202–1221.

Friston, K.J., Litvak, V., Oswal, A., Razi, A., Stephan, K.E., van Wijk, B.C.M., Ziegler, G., Zeidman, P., 2016. Bayesian model reduction and empirical Bayes for group (DCM) studies. NeuroImage 128, 413–431.
Goel, R., Nakagome, S., Rao, N., Paloski, W.H., Contreras-Vidal, J.L., Parikh, P.J., 2019. Fronto-parietal brain areas contribute to the online control of posture during a continuous balance task. Neuroscience 413, 135–153.
Hinton, D.C., Thiel, A., Soucy, J.-P., Bouyer, L., Paquette, C., 2019. Adjusting gait step-by-step: brain activation during split-belt treadmill walking. NeuroImage 202, 116095.
Jahn, K., Deutschländer, A., Stephan, T., Kalla, R., Wiesmann, M., Strupp, M., Brandt, T., 2008. Imaging human supraspinal locomotor centers in brainstem and cerebellum. NeuroImage 39 (2), 786–792.
Jeannerod, M., 1995. Mental imagery in the motor context. Neuropsychologia 33 (11), 1419–1432.
Jeannerod, Marc. (2001). Neural simulation of action: a unifying mechanism for motor cognition. *NeuroImage* https://doi.org/10.1006/nimg.2001.0832.
la Fougère, C., Zwergal, A., Rominger, A., Förster, S., Fesl, G., Dieterich, M., Brandt, T., Strupp, M., Bartenstein, P., Jahn, K., 2010. Real versus imagined locomotion: a [18F]-FDG PET-fMRI comparison. NeuroImage 50 (4), 1589–1598.
Lulé, D., Diekmann, V., Kassubek, J., Kurt, A., Birbaumer, N., Ludolph, A.C., Kraft, E., 2007. Cortical plasticity in amyotrophic lateral sclerosis: motor imagery and function. Neurorehabilitation Neural Repair 21 (6), 518–526.
Maidan, I., Rosenberg-Katz, K., Jacob, Y., Giladi, N., Deutsch, J.E., Hausdorff, J.M., Mirelman, A., 2016. Altered brain activation in complex walking conditions in patients with Parkinson's disease. Parkinsonism Relat. Disord. 25, 91–96.
Malouin, F., Richards, C.L., Jackson, P.L., Dumas, F., Doyon, J., 2003. Brain activations during motor imagery of locomotor-related tasks: a PET study. Hum. Brain Mapp. 19 (1), 47–62.
Manto, M., Huisman, T.A.G.M., 2018. The cerebellum from the fetus to the elderly: history, advances, and future challenges. *Handb. Clin. Neurol.* https://doi.org/10.1016/B978-0-444-64189-2.00027-5.
Martino, G., Ivanenko, Y.P., Serrao, M., Ranavolo, A., d'Avella, A., Draicchio, F., Conte, C., Casali, C., Lacquaniti, F., 2014. Locomotor patterns in cerebellar ataxia. J. Neurophysiol. 112 (11), 2810–2821.
Matsumura, M., Nambu, A., Yamaji, Y., Watanabe, K., Imai, H., Inase, M., Tokuno, H., Takada, M., 2000. Organization of somatic motor inputs from the frontal lobe to the pedunculopontine tegmental nucleus in the macaque monkey. Neuroscience 98 (1), 97–110.
Meier, J.M., Burgh, H.K., Nitert, A.D., Bede, P., Lange, S.C., Hardiman, O., Berg, L.H., Heuvel, M.P., 2020. Connectome-based propagation model in amyotrophic lateral sclerosis. Ann. Neurol. 87 (5), 725–738.
Middleton, F.A., Strick, P.L., 2000. Basal ganglia and cerebellar loops: motor and cognitive circuits. Brain Res. Rev. https://doi.org/10.1016/S0165-0173(99)00040-5.
Mori, F., Nakajima, K., 2010. Cortical control in locomotion. Brain Nerve.
Musienko, P.E., Zelenin, P.V., Lyalka, V.F., Gerasimenko, Y.P., Orlovsky, G.N., Deliagina, T.G., 2012. Spinal and supraspinal control of the direction of stepping during locomotion. J. Neurosci. 32 (48), 17442–17453.
Pool, E.-M., Rehme, A.K., Fink, G.R., Eickhoff, S.B., Grefkes, C., 2013. Network dynamics engaged in the modulation of motor behavior in healthy subjects. NeuroImage 82, 68–76.
Pradat, P.-F., Bruneteau, G., Munerati, E., Salachas, F., Le Forestier, N., Lacomblez, L., Lenglet, T., Meininger, V., 2009. Extrapyramidal stiffness in patients with amyotrophic lateral sclerosis. Mov. Disord. 24 (14), 2143–2148.
Proudfoot, M., Bede, P., Turner, M.R., 2019. Imaging cerebral activity in amyotrophic lateral sclerosis. *Front. Neurol.* https://doi.org/10.3389/fneur.2018.01148.
Quinn, C., Edmundson, C., Dahodwala, N., Elman, L., 2020. Reliable and efficient scale to assess upper motor neuron disease burden in amyotrophic lateral sclerosis. Muscle Nerve 61 (4), 508–511.
Rowe, J.B., Hughes, L.E., Barker, R.A., Owen, A.M., 2010. Dynamic causal modelling of effective connectivity from fMRI: are results reproducible and sensitive to Parkinson's disease and its treatment? NeuroImage 52 (3), 1015–1026.
Shaikh, A.G., Meng, H., Angelaki, D.E., 2004. Multiple reference frames for motion in the primate cerebellum. J. Neurosci. https://doi.org/10.1523/JNEUROSCI.0109-04.2004.
Simon, N.G., Lin, C.-Y., Lee, M., Howells, J., Vucic, S., Burke, D., Kiernan, M.C., 2015. Segmental motoneuronal dysfunction is a feature of amyotrophic lateral sclerosis. Clin. Neurophysiol. 126 (4), 828–836.
Takakusaki, K., 2017. Functional neuroanatomy for posture and gait control. *J. Mov. Disord.* 10 (1), 1–17.
Takakusaki, K., Tomita, N., Yano, M., 2008. Substrates for normal gait and pathophysiology of gait disturbances with respect to the basal ganglia dysfunction. J. Neurol. 255 (S4), 19–29.
Tessitore, A., Esposito, F., Monsurrò, M.R., Graziano, S., Panza, D., Russo, A., Migliaccio, R., Conforti, F.L., Morrone, R., Quattrone, A., Di Salle, F., Tedeschi, G., 2006. Subcortical motor plasticity in patients with sporadic ALS: an fMRI study. Brain Res. Bull. 69 (5), 489–494.
Tjernström, F., Fransson, P.-A., Patel, M., Magnusson, M., 2010. Postural control and adaptation are influenced by preceding postural challenges. Exp. Brain Res. 202 (3), 613–621.
Tu, S., Menke, R.A.L., Talbot, K., Kiernan, M.C., Turner, M.R., 2018. Regional thalamic MRI as a marker of widespread cortical pathology and progressive frontotemporal involvement in amyotrophic lateral sclerosis. J. Neurol. Neurosurg. Psychiatry 89 (12), 1250–1258.
Visser, J.E., Bloem, B.R., 2005. Role of the basal ganglia in balance control. *Neural Plasticity* 12 (2-3), 161–174.
Yanagihara, D., Udo, M., 1994. Climbing fiber responses in cerebellar vermal Purkinje cells during perturbed locomotion in decerebrate cats. Neurosci. Res. 19 (2), 245–248.
Zeidman, P., Jafarian, A., Seghier, M.L., Litvak, V., Cagnan, H., Price, C.J., Friston, K.J., 2019. A guide to group effective connectivity analysis, part 2: second level analysis with PEB. NeuroImage 200, 12–25.